Monolayer Organization Modeling Using Molecular Dynamics

S. Rovillard,† E. Perez,‡ R. Ionov,§ M. Voué,† and J. De Coninck*,†

Université De Mons-Hainaut, Laboratoire de Modélisation Moléculaire, 20, Place du Parc, B-7000 Mons, Belgium, Ecole Normale Superieure, Laboratoire de Physique Statistique, 24, rue Lhommond, F-75231 Paris Cedex 05, France, and Technical University, Institute of Applied Physics, BG- 1156 Sofia, Bulgaria

Received August 4, 1998. In Final Form: December 21, 1998

Many experiments have highlighted the existence of an unexpected long-range attractive force between two hydrophilic or hydrophobic monolayers, immersed in water or in nonaqueous solvents. The origin of this attraction has not been discovered yet. A mechanism responsible for these forces may be an interaction between ordered domains of the two close monolayers. The occurrence and characteristics of such domains are related to the nature of their constituting molecules and also their structural organization. We present here a molecular analysis, via molecular dynamics simulations, of ordered domains within a monolayer. We investigate the dependence between the characteristics of the domains and both the length of the molecules and the layer density.

1. Introduction

Monolayers of lipid or other amphiphilic molecules can exist in different phase states, such as disordered, condensed liquid, or 2D crystalline solid state. This has been shown experimentally in the past few years by X-ray diffraction at small angle and Brewster angle microscopy. The molecules aggregate at the interface and usually form domains. The internal structure, size, and orientation of such domains can influence strongly the properties of the monolayer and the interactions between such monolayers.

A long-range attractive force between hydrophobic surfaces immersed in water has been measured using a surface forces apparatus.[1] Each mica surface was hydrophobized by a Langmuir−Blodgett deposition of a lipid monolayer. Such forces have also been studied by atomic force microscopy.[2] There is experimental evidence that the length of the molecules adsorbed and the temperature influence the magnitude and the range of the attractive force. The phenomenon was observed between surfaces in water, but it also occurs in nonaqueous solvents such as ethylene glycol. The structural properties of water therefore cannot be the unique factor responsible for these forces, which are orders of magnitude larger than the value expected from van der Waals interactions. These forces only appear when the monolayers are in a solid state, proving that the detailed structure of the surface plays a key role. Similar forces were also observed with mica surfaces bearing lipid layers functionalized by the DNA bases deoxyadenosine and thymidine.[3,4] There, the surfaces were hydrophilic and uncharged but the long-range attraction could also be attributed to the same type of mechanism, that is, ordering in the lipid monolayers.

The occurrence of the long-range attractive forces between two layers may result from an interaction between polarized domains of the monolayers on both surfaces. To identify the mechanism leading to the formation of these domains is however a very difficult problem from a purely experimental point of view.[5]

In this paper, we perform numerical simulations to describe how the molecular aggregation and domain formation within a monolayer depend on its density and the length of its molecules. Up to now, most studies of this kind focused on the order between the rodlike carboxyl chains of the monolayer.[6] We are interested in studying the aggregation and ordering within the ringlike groups. The domains are characterized by their size and their structural order. These domains would induce very strong dipolar interactions and could be responsible for the long-range attraction between lipid monolayers. Our idea is to find the physical mechanism leading to domain formation using molecular modeling. Is the aggregation due to the steric effects (e.g. stacking of disk platelets) or to the molecular dipolar interaction or p−p interactions?[9,10] At this stage, we indeed ignore for simplicity the dipolar effects. We build in fact a monolayer using molecular dynamics, and we follow the evolution of domains versus time. What we wanted to study in this paper is if the steric effects can already induce some ordering within the

* Corresponding author.
† Universite De Mons-Hainaut.
‡ Ecole Normale Superieure.
§ Technical University.

(1) Israelachvili, J. N.; Adams, G. E. *J. Chem. Soc., Faraday Trans. 1* **1978**, *74*, 975−1001.
(2) Tsao, Y.-H.; Evans, D. F.; Wennerström, H. Long-Range Attractive Force Between Hydrophobic Surfaces Observed by Atomic Force Microscopy. *Science* **1993**, *262*, 547.
(3) Pincet, F.; Perez, E.; Bryant, G.; Lebeau, L.; Mioskowski, C. Long-Range Attraction between Nucleosides with Short-Range Specificity: Direct Measurements. *Am. Phys. Soc.* **1994**, *73*, 2780.
(4) Ionov, R.; De Coninck, J.; Angelova, A. On the origin of the long-range attraction between surface confined DNA bases. *Thin Solid Films* **1996**, *284−285*, 347−351.
(5) Angelova, A.; Ionov, R. Langmuir-Blodett Film Organization Resulting from Asymmetrical or Partial Types of Monolayer Transfer: Comparison for Amphiphiles of Different Geometrical Shapes. *Langmuir* **1996**, *12*, 5643−5653.
(6) Gao, J.; Rice, A. Intermediate ordering in a liquid supported monolayer: A molecular dynamics study. *J. Chem. Phys.* **1993**, *99* (9), 7020−7029.
(7) Dauber-Osguthorpe, P.; Roberts, V. A.; Osguthorpe, D. J.; Wolff, J.; Genest, M.; Hagler, A. T. *Protein: Struct., Funct. Genet.* **1988**, *4*, 31−47.
(8) Wilson, E. B.; Decius, J. C.; Cross, P. C. *Molecular Vibrations*; Dover: New York, 1980.
(9) Ionov, R.; Angelova, A. Discotic Multiyne Langmuir-Blodgett Films. 1. *J. Phys. Chem.* **1995**, *99*, 17593−17605.
(10) Angelova, A.; Ionov, R. Discotic Multiyne Langmuir-Blodgett Films. 2. *J. Phys. Chem.* **1995**, *99*, 17606−17615.

10.1021/la980976d CCC: $18.00
Published on Web 03/26/1999

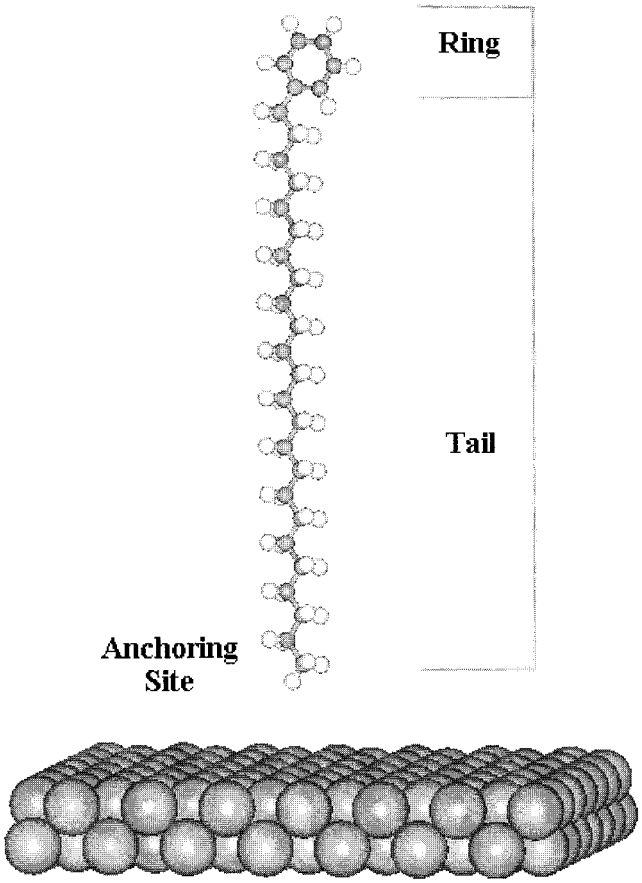

Figure 1. Template molecular system of our monolayers.

considered chains. If that is revealed to be true, as has been observed in the study, then there is no doubt that the dipole interactions will only enhance very strongly this structural ordering phenomenon.

The paper is organized as follows: Section 2 is devoted to the presentation of our model. The results are given in section 3. Concluding remarks are presented in section 4.

2. Model

Our monolayers are constituted by a set of N long chains ended by a ring. The chains are anchored by their end sp^3 carbon atom at a regular distance from a solid substrate. For convenience, we choose for the solid a piece of aluminum regular lattice. The aluminum nature of the substrate is by no mean important here. The distance between the substrate and the anchoring site of the chains corresponds to the equilibrium distance between an aluminum atom and a sp^3 carbon atom, that is to say, 0.455 nm. Figure 1 illustrates a typical molecule of the monolayer with a piece of the solid substrate.

The atoms of distinct molecules interact per pair (i, j) via a classical Lennard-Jones potential of the form

$$U_{LJ}(r_{ij}) = \frac{C_{ij}}{r_{ij}^{12}} - \frac{D_{ij}}{r_{ij}^{6}} \tag{1}$$

with $r_{ij} = |r_j - r_i|$ and the distance between atoms i and j, r, being a Cartesian coordinate. In our simulations, we have to consider five types of atoms: h stands for hydrogen atoms bonded to carbon atoms; c3 stands for carbon atoms bonded to three hydrogen atoms; c2 stands for carbon atoms bonded to two hydrogen atoms; cp stands for aromatic carbon atoms of the ring; al stands for aluminum atoms of the substrate.

Table 1. Lennard-Jones Parameters for the Different Species

atom type	C_i (kcal mol^{-1} Å^{12})	D_i (kcal mol^{-1} Å^6)	mass (amu)
h	7 108.4660	32.870 76	1.007 970
c2	1 981 049.2250	1125.998 00	12.011 150
c3	1 981 049.2250	1125.998 00	12.011 150
cp	2 968 753.3590	1325.708 10	12.011 150
al	11 422 865.0000	2282.966 06	26.982 000

Table 2. Bond-Stretching Potential Parameters

bonded atoms	l_0 (Å)	K_{str} (kcal mol^{-1} Å^{-2})
c2−c2	1.5260	322.7158
c2−c3	1.5260	322.7158
c2−h	1.1050	340.6175
c3−h	1.1050	340.6175
cp−h	1.0800	363.4164
cp−cp	1.3400	480.0000
cp−c2	1.5100	283.0924

The potential parameters C_{ij} and D_{ij} are those given by the consistent valence force field (CVFF)[7]

$$C_{ij} = \sqrt{C_i \cdot C_j}$$
$$D_{ij} = \sqrt{D_i \cdot D_j} \tag{2}$$

where C_i and D_i are defined in Table 1.

To save computational time, we have chosen a cutoff radius equal to 1.590 nm. If the distance between two atoms exceeds 1.590 nm, we do not compute the interaction. A higher cutoff radius would considerably increase the duration of the simulations and would be of no use in the results' accuracy.

We fix c3 atoms close to their initial positions by adding an extra energy term:

$$U_{fix} = K_{fix}(r - r_0)^2 \tag{3}$$

where $r - r_0$ is the deviation of the c3 atoms from their initial positions and $K_{fix} = 500$ kcal mol^{-1}Å^{-2}. The same potential is used to maintain the atomic organizational structure of the solid substrate. The atomic masses are fixed as described in Table 1, and we follow the time evolution of the system during 100 000 time steps of 0.52 fs. A "thermostat bath" technique allows the temperature of the system to fluctuate between 296 and 300 K. To minimize finite size effects, we chose periodic boundary conditions in the x and y directions; the z-axis being normal to the solid sheet.

To be able to reproduce the molecular characteristics, we add four potential intramolecular terms. A bond-stretching harmonic potential keeps the distance between neighboring atoms close to a reference value:

$$U_{str} = K_{str}(l - l_0)^2 \tag{4}$$

with l the distance between the two atoms of the considered bond and l_0 its reference value and where K_{str} is a potential coefficient. The different values of those parameters are described in Table 2 according to the nature of both bonded atoms.

A bending potential is used to fix the angle between adjacent bonds:

$$U_{bend} = K_{bend}(\theta - \theta_0)^2 \tag{5}$$

with θ and θ_0 the bond angle and its reference value. Table 3 lists the possible values for θ_0 and the bending potential coefficient K_{bend}.

Table 3. Bending Potential Parameters

bonded atoms	θ_0 (deg)	K_{bend} (kcal mol^{-1})
h−c2−h	106.4000	39.5000
h−c3−h	106.4000	39.5000
h−c2−c2	110.0000	44.4000
h−c2−c3	110.0000	44.4000
h−c2−cp	110.0000	44.4000
h−c3−c2	110.0000	44.4000
c2−c2−c2	109.5000	70.000
c2−c2−c3	109.5000	70.000
c2−c2−cp	110.5000	46.6000
cp−cp−cp	120.0000	90.0000
c2−cp−cp	120.0000	44.2000
h−cp−cp	120.0000	37.0000

Table 4. Dihedral Torsional Potential Parameters

bonded atoms (* can be any atom)	K_{tors} (kcal mol^{-1})	n	φ_0 (deg)
−c2−c2−	1.4225	3	0.0000
−c3−c2−	1.4225	3	0.0000
−cp−c2−	0.0000	2	0.0000
−cp−cp−	12.0000	2	180.0000

Table 5. Out-of-Plane Potential Coefficients

atom types						
1	2	3	4	K_{oop} (kcal mol^{-1})	n	χ_0 (deg)
cp	cp	cp	h	0.3700	2	180.0000
cp	cp	cp	c	0.3700	2	180.0000
cp	cp	cp	cp	0.3700	2	180.0000

A dihedral torsional potential is necessary between three adjacent bonds, to keep the planarity of the ring carbon atoms:

$$U_{tors} = K_{tors}[1 + \cos(n\varphi - \varphi_0)] \quad (6)$$

with φ and φ_0 the dihedral angle and its reference value, n a symmetry coefficient and K_{tors} a potential coefficient (see Table 4).

To end the molecular description, let us here mention that an out-of-plane contribution is computed, of the form

$$U_{oop} = K_{oop}[1 + \cos(n\chi - \chi_0)] \quad (7)$$

where χ and χ_0 are the out-of-plane "Wilson" angle[8] and its reference value and n and K_{oop} are symmetry and potential coefficients. See Table 5 for the values of these coefficients; "atom 2" is the central atom of the Wilson χ angle.

Given the coordinates of all the atoms, we can compute the force acting on them from the total potential. The motion of these atoms follows by integrating Newton's equations of motion.

3. Results

In our simulations, we have considered three different layer densities and four lengths of molecules. The system is constituted by 25 molecules anchored by their c3 carbon atoms. The anchoring sites define a squared mesh lattice. We have chosen three densities corresponding to three squared lattices of dimensions 0.445 nm × 0.445 nm, 0.486 nm × 0.486 nm, and 0.567 nm × 0.567 nm or, in other words, the following area per molecules: 0.198, 0.236, and 0.321 nm^2/mol. We have combined each of these three lattices with 25 molecules of 15 (C_7H_8), 24 ($C_{10}H_{14}$), 54 ($C_{20}H_{34}$), 84 ($C_{30}H_{54}$), or 144 ($C_{50}H_{94}$) atoms. A simulation will hereinafter be referred to by a letter and a number (l, f) with l corresponding to the monolayer density (a, 0.198 nm^2/mol; b, 0.236 nm^2/mol; c, 0.321 nm^2/mol) and f corresponding to the number of carbon atoms of the molecule (10, 20, 30, or 50).

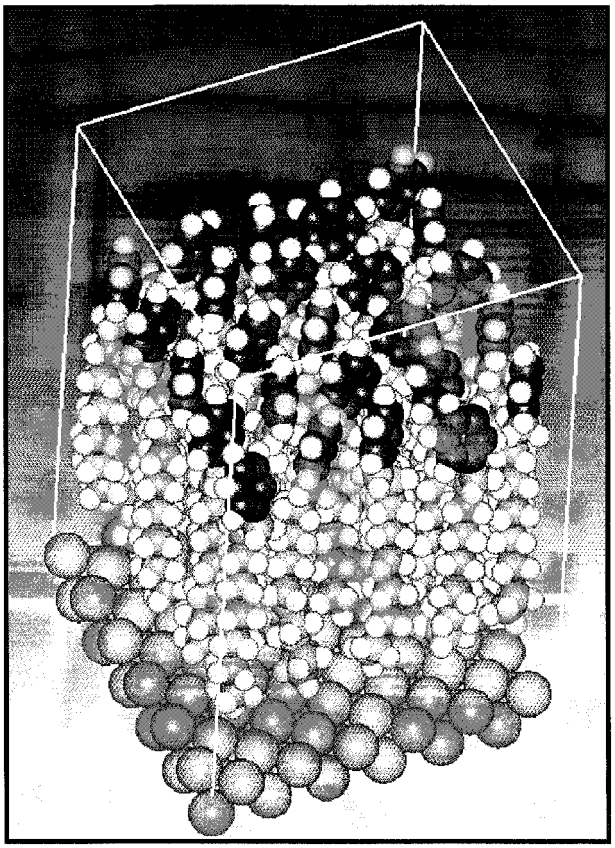

Figure 2. Typical snapshot (system (C, 20)).

We have carried out simulations with 100 molecules under periodic boundary conditions, to check the sensitivity of our results to the finite number of considered molecules. No significant changes have been seen.

We observe a tendency for the molecules to aggregate in clusters for small lattice spacing as illustrated by the snapshots given in Figure 2.

Let us now describe the procedure. The initial configuration is made by equilibrated individual molecules. We then let the system equilibrate to be sure that we have reached an equilibrium state. We therefore check the temporal stability of the potential and kinetic energies. Once the equilibrium plateau for all these variables has been reached, we study the ordering within the monolayer. We have also verified that we recover equivalent results for longer simulations. Typically, we have considered a few 500 000 time step simulations and their results are equivalent to the presented results in this paper. Figure 3 shows the stability of the average potential energy for simulations with 100 000 and 500 000 time steps.

The clusters of molecules can be characterized by two types of ordering: a spatial ordering related to the proximities of the head groups and an orientational ordering related to the orientation of the rings. Let us then define the variables we will use: (i) to each molecule, we associate a "CM pseudo-atom" defined as the center of mass of the ring atoms; (ii) to each ring is associated a unit order vector located at the CM and normal to the head plane.

For all the simulations, we first check if there are spatial clusters using the following procedure:

(1) We consider the "CM pseudo-atom" of the first molecule (CM1). To this first molecule is associated the cluster "1". We then measure the distances between CM1

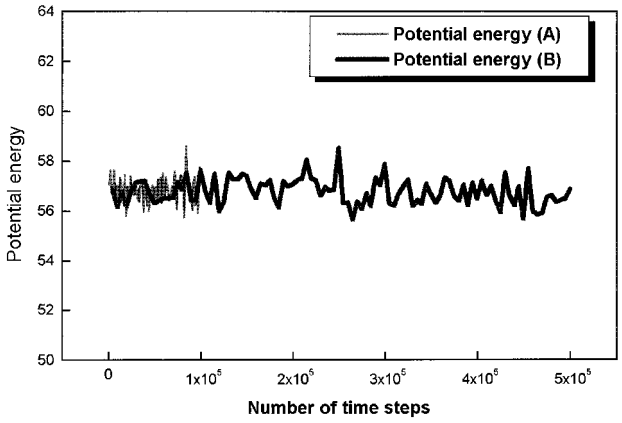

Figure 3. Evolution of the potential energy (in usual reduced units) versus the number of time steps for the system (b, 20). Two simulations have been considered: 100 000 (A) and 500 000 (B) time steps long.

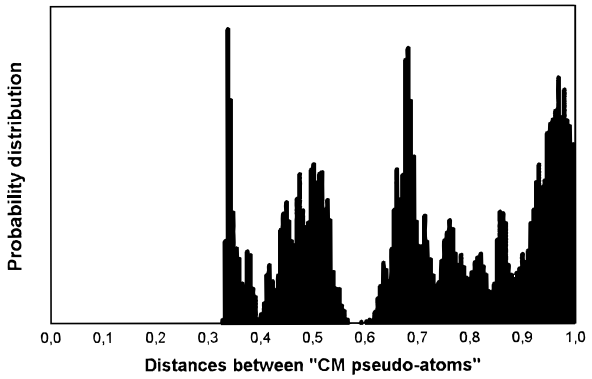

Figure 4. Time average evolution of the distribution of the distances between "CM pseudo-atoms" in nanometers for 10 C chains. The monolayer density is fixed at 0.236 nm^2/mol.

and all other CMs. If one of the distances is lower than the cluster reference distance (see below), the corresponding molecule is attached to the same cluster "1".

(2) We then jump to the second "CM pseudo-atom" of the first cluster and study if there are other "CM pseudo-atoms" within a sphere of radius equal to the cluster reference distance. If we find one, we incorporate it to the cluster "1", and so on.

(3) When we are unable to add a new atom to the cluster "1", we try to find a "CM pseudo-atom" not yet associated to the cluster "1"; this will be the starting point of cluster "2".

How can we choose the cluster reference distance?

If two molecules are trapped in a cluster, close to each other, the distance between them is inferred by the potential applied between their atoms. The potential we use (see section 2) is the classical Lennard-Jones potential. This potential leads to a minimum of energy for a distance between interacting cp atoms of 0.406 nm. We thus fix the cluster reference distance to that value of 0.406 nm. Indeed, if we obtain clusters for this minimal cutoff length, we will get even larger clusters for any larger cutoff distance. We have also checked that our results are not affected by small fluctuations (a few percents) around this value.

How can we describe an ordering phenomenon within the rings? During the simulation, we consider, for each cluster, the existence of stacks. If two rings of the same cluster are parallel (we admit a fluctuation of 2.5°), they belong to the same stack. Resulting is the average over the simulation time of the number of molecules per stack.

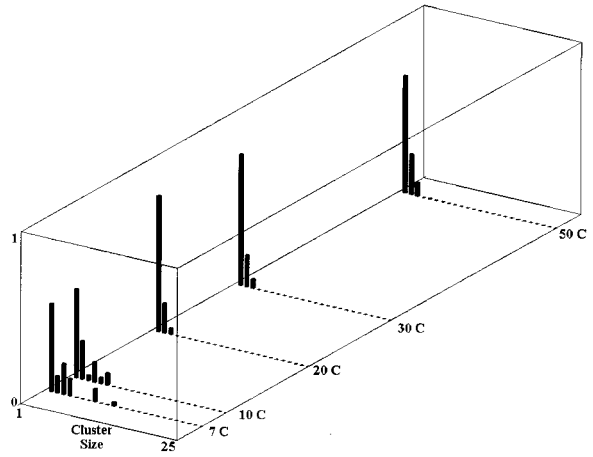

Figure 5. Cluster size probability distribution versus the number of carbon atoms (7C, 10C, 20C, 30C, or 50C) per molecule averaged over a period of time of 52 ps. The monolayer density is fixed at 0.236 nm^2/mol.

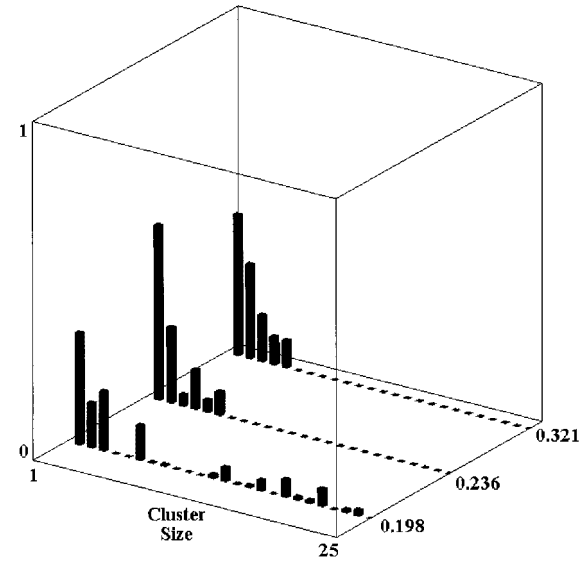

Figure 6. Cluster size probability distribution versus the monolayer density averaged over a period of time of 52 ps. The number of carbon atoms per molecule is fixed at 10.

We have also checked that this value of 2.5° could admit fluctuations of a few degrees without significant changes of the results.

During the simulation, various variables can be studied: (i) the time average of the distribution of the distances between the "CM pseudo-atoms" and (ii) the average number of molecules per cluster and stack.

Figure 4 shows the time average of the distribution of the distances between the "CM pseudo-atoms". The first maximum corresponds to the shortest possible distance between two rings, which is the distance between two adjacent heads in the same cluster. This graph confirms the validity of the choice of our cluster reference distance as 0.406 nm.

Figures 5−12 show respectively the probability distribution of the size of the clusters, the probability distribution of the size of the stacks, the evolution of the average size of the clusters, and the evolution of the average size of the stacks versus the number of carbon atoms of the molecules for the 0.486 nm lattice mesh or versus the density of the monolayer for molecules with 10 carbon atoms.

We observe that the cluster (or stack) size decreases with an increase of the chain length. For long chains (more

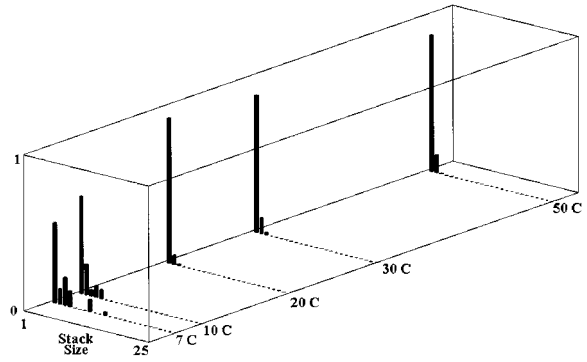

Figure 7. Stack size probability distribution versus the number of carbon atoms (10C, 20C, 30C, or 50C) per molecule, averaged over a period of time of 52 ps. The monolayer density is fixed at 0.236 nm^2/mol.

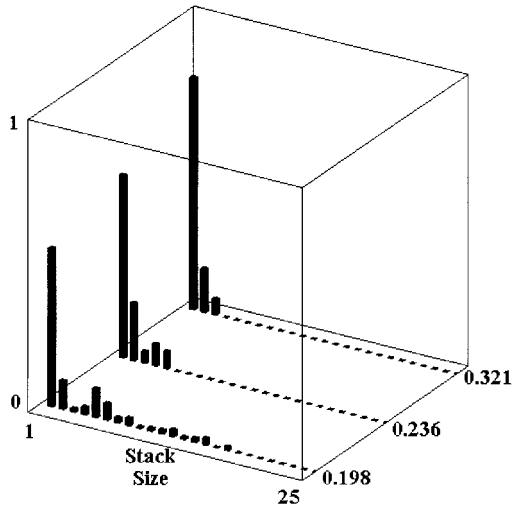

Figure 8. Stack size probability distribution versus the monolayer density, averaged over a period of time of 52 ps. The number of carbon atoms per molecule is fixed at 10.

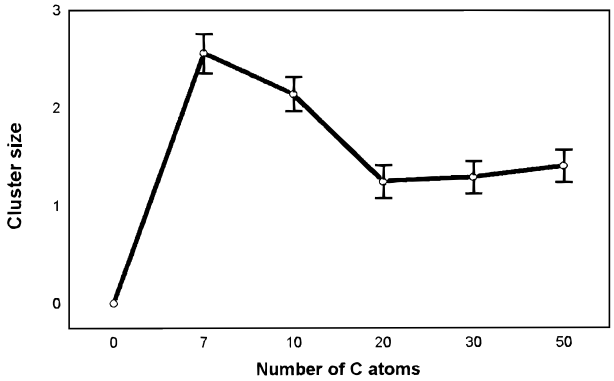

Figure 9. Mean cluster size versus the number of carbon atoms per molecule. The monolayer density is fixed at 0.236 nm^2/mol. The error bars correspond to one statistical deviation.

than 20 C atoms), the cluster sizes are smaller, due to entanglement between chains, as confirmed by snapshots of the different systems. Knowing that if the molecule is too small, there will be, according to our definition, no cluster or stack at all, that result implies that there is an optimal length for the ordering of the molecules. This may be understood as the result due to the competition between the energy of the cycles and the entropy of the chains. As expected, the average size of clusters and stacks decreases when increasing the spacing between the molecules, as given in the following figures.

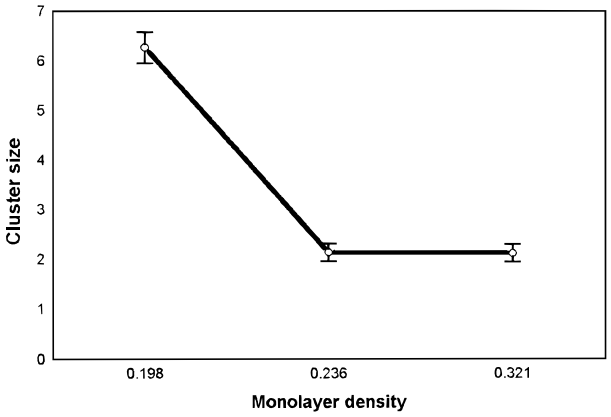

Figure 10. Mean cluster size versus the monolayer density. The number of carbon atoms per molecule is fixed at 10. The error bars correspond to one statistical deviation.

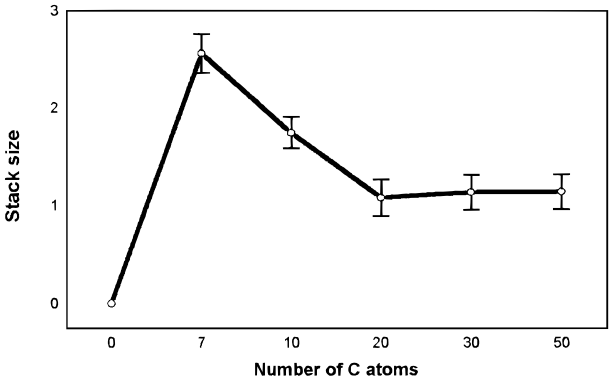

Figure 11. Mean stack size versus the number of carbon atoms per molecule. The monolayer density is fixed at 0.236 nm^2/mol. The error bars correspond to one statistical deviation.

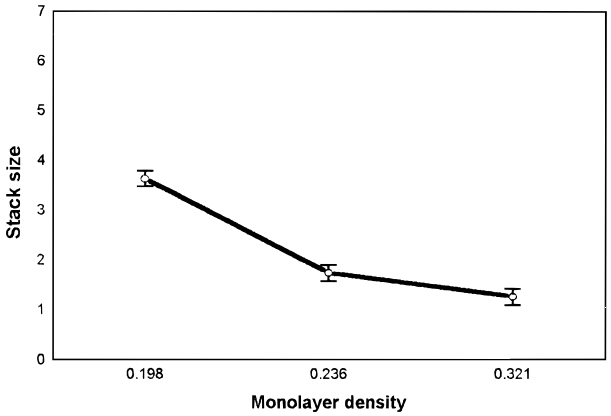

Figure 12. Mean stack size versus the monolayer density. The number of carbon atoms per molecule is fixed at 10. The error bars correspond to one statistical deviation.

We do not have explicitly introduced water molecules in our simulations, to save computational time. However, we expect an increase in the cluster and stack sizes due to the amphiphilic nature of the considered molecules. The hydrophilic ring groups attract the water molecules, whereas the hydrophobic tails are rejected by the solvent. To mimic this effect, we have carried out two additional simulations, in which the attractive part of the Lennard-Jones potential between the ring and tail atoms has been reduced by the factor 2.5. The other interaction parameters were not changed. Figure 13 shows the observed significative increase in the average cluster size for those two new simulations. The parameters were set to 0.236 nm^2/

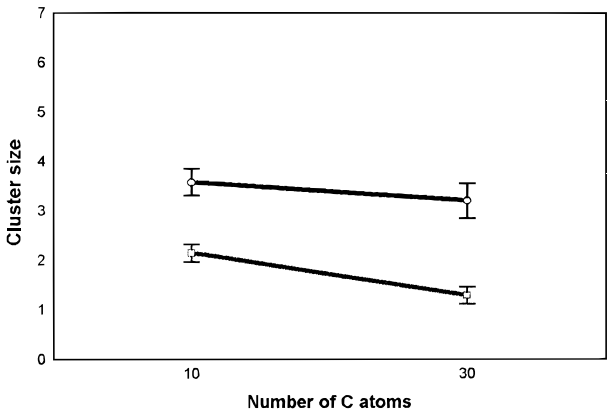

Figure 13. Mean cluster size versus the number of carbon atoms per molecule. The monolayer density is fixed at 0.236 nm^2/mol. The upper curve is related to simulations with decreased interaction between the ring and tail atoms, to mimic some solvent effect. The error bars correspond to one statistical deviation.

mol for the monolayer density and 10 and 30, respectively, for the number of C atoms of the molecules.

4. Concluding Remarks

Using molecular dynamics simulations, we have shown that there exist clusters of cycles which are ordered taking only into account Lennard-Jones interactions. That is to say that the steric effects can already induce some ordering within the monolayers. Knowing that we have also induced dipolar effects for the studied lipid layers, this shows that there will be a strong effective ordering of the cycles in the experiment. Our study thus supports the existence of such domains within the considered monolayers, as already conjectured in ref 4. These domains will thus increase the interaction forces between the two considered plates. That this effect is the only one required to understand the observations remains however an open question. Further studies would be necessary to consider in detail the effect of dipole−dipole and p−p interactions within the ring region. The fact that we have observed an optimal length for this ordering would be interesting to confirm experimentally. Let us also here stress that we have shown that the amphiphilic character of the considered molecules some solvents will enhance this ordering of rings. More realistic simulations including such dipolar interactions are now under consideration to estimate quantitatively the associated increase of forces.

Acknowledgment. This research has been partially supported by the European Community and the Région Wallonne (FIRST, Grant 9713448) and in the program Feder−Objective I.

LA980976D